Environmental Modelling & Software 26 (2011) 804–816

Contents lists available at ScienceDirect

Environmental Modelling & Software

journal homepage: www.elsevier.com/locate/envsoft

Component-based development and sensitivity analyses of an air pollutant dry deposition model

Satoshi Hirabayashi[a], Charles N. Kroll[b,*], David J. Nowak[c]

[a] The Davey Tree Expert Company, 5 Moon Library, SUNY College of Environmental Science and Forestry, Syracuse, New York 13210, United States
[b] Environmental Resources Engineering, SUNY College of Environmental Science and Forestry, 1 Forestry Drive, 402 Baker Laboratory, Syracuse, New York 13210, United States
[c] USDA Forest Service, Northeastern Research Station, 5 Moon Library, SUNY College of Environmental Science and Forestry, Syracuse, New York 13210, United States

ARTICLE INFO

Article history:
Received 30 August 2009
Received in revised form
22 November 2010
Accepted 28 November 2010
Available online 19 January 2011

Keywords:
Air pollutant
Dry deposition
Component-based model
UFORE
Sensitivity analysis

ABSTRACT

The Urban Forest Effects-Deposition model (UFORE-D) was developed with a component-based modeling approach. Functions of the model were separated into components that are responsible for user interface, data input/output, and core model functions. Taking advantage of the component-based approach, three UFORE-D applications were developed: a base application to estimate dry deposition at an hourly time step, and two sensitivity analyses based on Monte Carlo simulations with a Latin hypercube sampling (LHS-MC) and a Morris one-at-a-time (MOAT) sensitivity test. With the base application, dry deposition of CO, NO_2, O_3, PM10, and SO_2 in the city of Baltimore was estimated for 2005. The sensitivity applications were performed to examine UFORE-D model parameter sensitivity. In general, dry deposition velocity was sensitive to temperature and leaf area index (LAI). Temperature had a non-linear effect on all pollutants, while LAI was important to NO_2 deposition with a nearly linear effect. PAR and wind speed had limited effects on dry deposition of all pollutants; dry deposition was affected by PAR and wind speed only up to their threshold values. The component-based approach allows for seamless integration of new model elements, and provides model developers with a platform to easily interchange model components.

Software availability

Name of software: UFORE-D
Developer: Satoshi Hirabayashi, The Davey Tree Expert Company, 5 Moon Library, SUNY-ESF, 1 Forestry Drive, Syracuse, NY 13210
Tel.: +1 315 448 3201
Fax: +1 315 448 3216
E-mail: satoshi.hirabayashi@davey.com
First available: 2011 (integrated with i-Tree Eco)
Hardware required: PC running Windows XP or later
Software required: None
Program language: Visual Basic
Cost: Will be freely downloadable from http://www.itreetools.org/ in 2011.

1. Introduction

Environmental computer models are traditionally developed as closed monolithic systems (Bian, 2000; He et al., 2002). Individual research groups develop models suited for their purposes within their development platforms or modeling frameworks. Such models typically allow users to access the model only through input and output data, with no controls over the core model elements. When the models are released into the public domain these limitations become an issue for users who wish to make changes to the model. New applications are often built upon existing public domain models, or existing models are integrated into larger modeling frameworks. Such tasks often require users to learn and modify the model source code, which can be hard due to differences in programming languages, software architecture, or modeling frameworks. Data for the models are traditionally stored in a text file; however, new data storage schemes have become popular for improved handling of large amounts of data. To introduce new data formats into existing models, the model typically must be modified at the source code level. The lack of reusability and flexibility in the closed monolithic models create duplicated efforts, resulting in wasted time and energy.

The Urban Forest Effects-Deposition model (UFORE-D) is a public domain computer program widely used to quantify dry deposition (i.e. pollution removal during non-precipitation periods) to forest canopies in urban areas in North America (Nowak et al., 1998, 2000, 2006; Nowak and Crane, 2000; Deutsch et al., 2005; Currie and Bass, 2008). Because UFORE-D is a closed system, implemented as a large

* Corresponding author. Tel.: +1 315 470 6699; fax: +1 315 470 5968.
E-mail addresses: satoshi.hirabayashi@davey.com (S. Hirabayashi), cnkroll@esf.edu (C.N. Kroll), dnowak@fs.fed.us (D.J. Nowak).

1364-8152/$ – see front matter © 2010 Elsevier Ltd. All rights reserved.
doi:10.1016/j.envsoft.2010.11.007

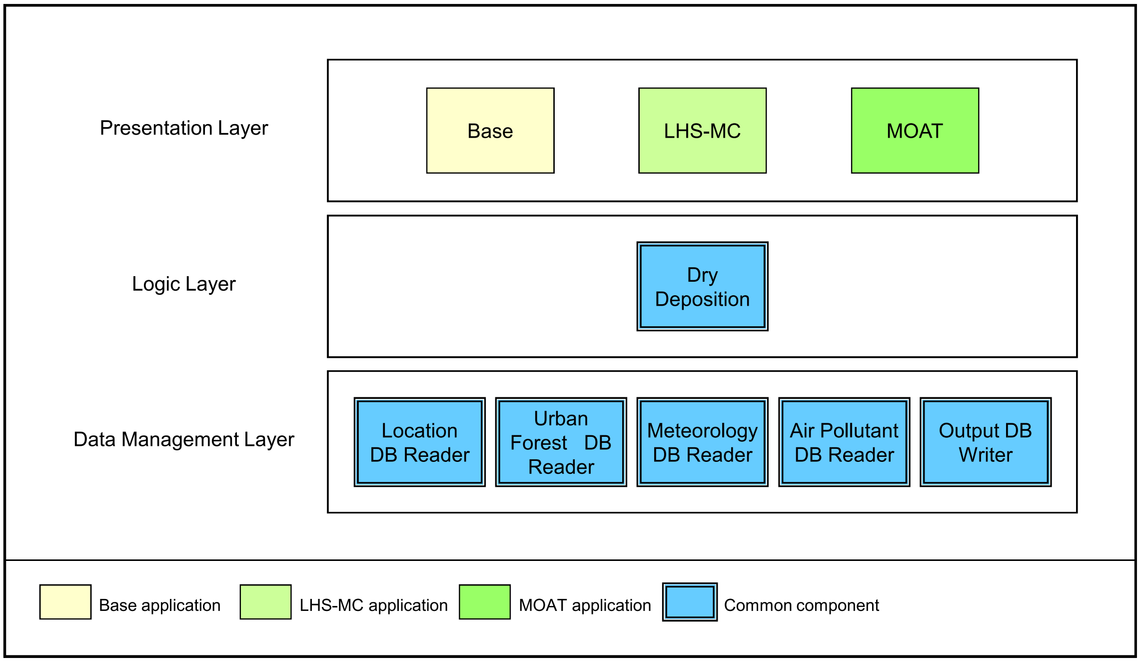

Fig. 1. Component structure of UFORE-D applications.

code written in SAS (Statistical Analysis Software), it is difficult for users to reuse UFORE-D for new applications. Furthermore, since the data format of UFORE-D are limited to text or SAS binary formats, employing different data formats such as a relational database requires modifications in the source codes.

These modeling problems may be overcome by employing Component-Based Software Engineering (CBSE) concepts. CBSE is an emerging paradigm in software development and is seen as a major new direction in the post object-oriented approach era (Bian, 2000). CBSE breaks the executable model code into separate pieces or components. A component comes packaged as a binary code ready to perform certain tasks for the entire model. Components connect to each other at run time to form a complete model. CBSE requires a binary architecture standard to regulate how components interact at run time (Argent, 2004). A widely used standard is the Component Object Model (COM) that Microsoft introduced for the Windows platform (Chappell, 1996). The use of components allows component transplanting, or the so-called 'plug and play' approach. While maintaining model integrity, a component of the model can be easily replaced with a new component. For instance, if data input/output functions are developed as components, a format change of the data requires replacing only these components. A component that performs model core functionality can be easily reused in other model applications. Even models developed in different frameworks can be readily merged if the frameworks comply with a CBSE standard such as COM. Thus, component-based approaches can drastically enhance the reusability and interoperability of environmental computer models.

In this study, development of UFORE-D with COM technology is reported. The developed components can collectively perform the same dry deposition modeling functions the original UFORE-D offers. As a case study, the dry deposition of five criteria air pollutants (CAPs), carbon monoxide (CO), nitrogen dioxide (NO_2), ozone (O_3), particulate matter less than 10 microns (PM10), and sulfur dioxide (SO_2), are quantified in Baltimore, MD in 2005.

In environmental model building processes, examining sensitivity of a model to changes in its parameters and inputs is an important model evaluation exercise. Sensitivity analyses allow one to gain knowledge of how the modeled system functions and to identify parameters of the model whose values need to be specified more accurately (Barnsley, 2007). Historically, sensitivity analyses have been performed in the development of environmental models (Liepmann and Stephanopoulos, 1985; MacKerron and Waister, 1985; Caton et al., 1999; Hermann et al., 2002; Weiler, 2005; Pohlert et al., 2007) including air pollutant models (Anfossi et al., 1996; Smith et al., 2000; Simpson et al., 2003; Wu et al., 2003; MacDougall et al., 2005; Ziehn and Tomlin, 2008; Mészáros et al., 2009). A variety of sensitivity analysis techniques have been proposed and reviewed in the literature (Hamby, 1994; Campolongo and Saltelli, 1997; Saltelli et al., 2000; Ravalico et al., 2005; Norton, 2008).

In the current study, two sensitivity analysis applications of COM-based UFORE-D are performed by reusing developed COM components. Development of these two applications exemplifies the components' transplantability and reusability. Through this exercise, the UFORE-D model is run for a wide range of model parameters that are representative of many vegetation and weather conditions observed throughout the United States, and the parameters the model is most sensitive to are identified.

2. Component and application design

Information systems are conceptually designed around three layers: presentation, logic, and data management (Alonso et al., 2004). The presentation layer provides a user interface and an overall control of applications. The logic layer controls a system's functionality by performing detailed processing. The data management layer handles data access and management. This architecture was adopted in this study to efficiently separate functionalities of UFORE-D into components that are responsible for specific tasks.

The developed components in the three layers are illustrated in Fig. 1. The five components in the data management layer, the Dry Deposition component in the logic layer, and the Base component in the presentation layer are assembled to perform the same functions as the original UFORE-D. Two more applications, Monte Carlo with Latin hypercube sampling (LHS-MC) and Morris one-at-a-time (MOAT) sensitivity analyses, which can perform a global sensitivity analysis of UFORE-D, are also developed. For these applications, components in the logic and data management layers are all reused; only components in the presentation layer are replaced.

COM components are generally developed with Microsoft Visual Studio, an integrated development environment (IDE) that includes features for editing, compiling, linking, deploying, and debugging software. Visual Basic (VB) 6.0 is used in this study. Components in the presentation layer are compiled into standard executables, while components in the logic and data management layers are compiled into ActiveX dynamic link libraries (DLLs). The standard executables are COM clients that get a pointer to a COM server and use its services by calling the methods of its interfaces. The DLLs are COM server components that provide services to clients in the form of COM interface implementations (MSDN, 2009). Design and functions of each component are explained in the next sections.

2.1. Data read/write components

UFORE-D takes a variety of data as its input and quantifies dry deposition of air pollutants in a city. Input data includes location related information, urban forest information, hourly meteorology and air pollutant concentration data. The location information includes time zone, latitude, longitude, and leaf-on and leaf-off dates. Urban forest characteristics include the maximum leaf area index (LAI) during the leaf-on season, tree coverage, and evergreen canopy percentages that can be used to approximate the minimum LAI during the leaf-off season. LAI is defined as the total area of leaves (one-sided) per unit ground surface area projected on the horizontal datum (NASA, 2009). UFORE-D outputs hourly results as well as summaries for longer periods. These data are stored in either text or SAS binary files in the original UFORE-D, while all data are stored in Microsoft Access databases in this study. With the relational database management functions and the structured query language (SQL) that Access offers, data extraction and summarization needed in the applications of this study can be effectively and efficiently achieved.

Using the city name and code as keys, the Location Database (DB) Reader and the Urban Forest DB Reader components issue an SQL command to the corresponding Access database to extract records for a specific city. Using SQL commands, the Meteorology DB Reader and the Air Pollutant DB Reader components offer flexibility for extracting records from the corresponding Access databases. Hourly records extracted can be specified for a certain period of hours in either a specific month or a period of Julian dates. In addition, these components calculate statistics (mean, minimum, maximum, and standard deviation) of data fields in the extracted records. Similarly, the Output DB Writer component provides several methods to output results, including hourly, daily, monthly, leaf-on and leaf-off season results, and annual summaries, into the corresponding Access databases.

2.2. Dry deposition component

The Dry Deposition component performs UFORE-D's core function, in which hourly dry deposition of CO, NO_2, O_3, PM10 and SO_2 is estimated with hourly meteorological and pollutant measurements, location information, and urban forest parameters. A brief model description is included below. Readers are referred to Hirabayashi et al. (2010) for a more complete description of the model.

Pollutant flux, F (g m^{-2} s^{-1}), is estimated as a product of the dry deposition velocity, V_d (m s^{-1}), and the air pollutant concentration, C (g m^{-3}):

$$F = V_d \cdot C \tag{1}$$

V_d is estimated as the inverse of the sum of resistances to pollutant transport (Baldocchi et al., 1987):

$$V_d = (R_a + R_b + R_c)^{-1} \tag{2}$$

where R_a represents air movement resistance in the crown space (aerodynamic resistance), R_b represents transfer resistance through the boundary layer immediately adjacent to canopy surfaces (quasi-laminar boundary layer resistance), and R_c represents the chemical and biological absorption capacity of the canopy surfaces (canopy resistance). R_a is calculated as (Killus et al., 1984):

$$R_a = \frac{u(z)}{u_*^2} \tag{3}$$

where $u(z)$ is the mean wind speed at height z, and u_* is the friction velocity calculated as a function of $u(z)$, roughness length, displacement length, and temperature, depending upon atmospheric stability (Venkatram, 1980; Dyer and Bradley, 1982; Killus et al., 1984; van Ulden and Holtslag, 1985; US EPA, 1995). R_b is calculated as (Pederson et al., 1995):

$$R_b = 2(Sc)^{2/3}(Pr)^{-2/3}(ku_*)^{-1} \tag{4}$$

where Sc is the Schmidt number, Pr is the Prandtl number, and k is the von Karman constant (=0.41).

Hourly R_c for NO_2, O_3, and SO_2 is calculated based on a hybrid of the big-leaf and multilayer canopy deposition models (Baldocchi et al., 1987; Baldocchi, 1988; Norman, 1980). R_c depends on four components: stomatal resistance (r_s), mesophyll resistance (r_m), cuticular resistance (r_t), and soil resistance (r_{soil}):

$$\frac{1}{R_c} = \frac{1}{r_s + r_m} + \frac{1}{r_t} + \frac{1}{r_{soil}} \tag{5}$$

r_m was set to 10 s m^{-1} for O_3 (Hosker and Lindberg, 1982), and 0 s m^{-1} for SO_2 (Wesely, 1989). r_m for NO_2 was set to 100 s m^{-1} (Hosker and Lindberg, 1982) to account for the difference between water vapor and NO_2 transport within mesophyll air spaces, and to ensure the V_d calculated was in the typical range reported by Lovett (1994). r_t was set to 20,000 s m^{-1} for NO_2 based upon Wesely (1989) assuming mixed forest in midsummer, and calculated as 10,000 s m^{-1} for O_3, and 8000 s m^{-1} for SO_2 to account for the typical variation in r_t exhibited among the pollutants (Taylor et al., 1988; Lovett, 1994). r_{soil} was set to 2000 s m^{-1} (Meyers and Baldocchi, 1993). Derivation of stomatal conductance, g_s, the inverse of r_s, is based on its link to leaf photosynthesis. g_s can be expressed as a function of net leaf photosynthesis (A), leaf surface relative humidity (rh), and the leaf surface CO_2 concentration (C_s) (Collatz et al., 1991; Leuning, 1990; Baldocchi, 1994):

$$g_s = \frac{mArh}{C_s} + b' \tag{6}$$

The coefficient m is a dimensionless slope (=10) and b' is the zero intercept when A is equal to or less than zero (=0.02 mol m^{-2} s^{-1}). A can be expressed as (Farquhar et al., 1980; Harley et al., 1992):

$$A = V_c - 0.5V_o - R_d \tag{7}$$

V_c and V_o are the carboxylation and oxygenation rate of CO_2 exchange between the leaf and the atmosphere, respectively. R_d is the dark respiration rate of the CO_2 exchange. A is a function of PAR, temperature, relative humidity, and wind speed. An analytical solution of A is described in detail in Baldocchi (1994). While earlier studies by Farquhar et al. (1980), Norman (1980), Leuning (1990), Collatz et al. (1991), and Harley et al. (1992) related the photosynthesis (A) by C3 grasses to g_s, later studies by Harley and Baldocchi (1995), Baldocchi and Harley (1995), Wilson et al. (2001), and Baldocchi and Wilson (2001) parameterized the model for C3 trees. UFORE-D was parameterized for trees based on these later studies. C_s can be expressed as (Baldocchi, 1994):

Table 1
Summary statistics of the UFORE-D input parameters for LHC-MC analysis.

Parameter	Minimum	Mean	Maximum	SD
LAI	2.5	5.8	10	1.7
PAR ($W m^{-2}$)	38.6	296.8	503.8	132.2
Pressure (hPa)	984.6	1011.4	1037.1	8.1
Relative humidity (%)	15.6	53.2	100.0	18.4
Temperature (°C)	−7.8	16.5	34.5	10.7
Wind speed ($m s^{-1}$)	0.5	4.1	11.6	2.3

$$C_s = C_a - \frac{A}{g_b} \tag{8}$$

C_a is atmosphere's CO_2 concentration (set to the global annual mean of 380 ppm in 2005 (NOAA, 2010)). Note that the CO_2 concentration in the atmosphere is increasing continuously (NOAA, 2010) and urban areas tend to have higher CO_2 concentrations due to human activities (Vitousek et al., 1997; Pataki et al., 2003). Higher CO_2 concentrations may decrease g_s, which leads to a decrease in the air pollutant flux due to the dry deposition (Baldocchi, 1994; Wu et al., 2003). g_b is conductance across the laminar boundary layer of a leaf, and a reciprocal of the sum of R_a and R_b for CO_2 exchange.

To represent r_s for the canopy level from r_s for the individual leaf level, Norman's (1980) canopy radiation transfer/interception model is employed. In this approach the canopy is divided into N layers of equal leaf area index increments (ΔLAI) and each canopy layer is divided into two classes of leaves: sunlit and shaded. In the jth layer, stomatal conductances calculated separately for sunlit and shaded leaves ($g_{s,sun,j}$ and $g_{s,shade,j}$, respectively) and combined according to the fraction of sunlit and shaded leaf area indices ($LAI_{sun,j}$ and $LAI_{shade,j}$, respectively) provide $g_{s,j}$. The summation of $g_{s,j}$ for the N layers provides the g_s for the entire canopy.

Table 2
Annual estimates of air pollution removal by total tree canopy cover and per unit tree canopy cover in Baltimore in 2005.

Air pollutant	Total pollution removal (t)		Pollution removal per unit tree cover ($g m^{-2}$)	
	Total	Range	Total	Range
CO	7	na	0.2	na
NO_2	61	23–81	1.4	0.5–1.9
O_3	199	44–275	4.7	1.1–6.4
PM10	136	53–212	3.2	1.2–5.0
SO_2	44	17–76	1.0	0.4–1.8
Total	447	137–645	10.5	3.2–15.1

$$g_s = \sum_{j=1}^{N} g_{s,j} = \sum_{j=1}^{N}\left(g_{s,sun,j}LAI_{sun,j} + g_{s,shade,j}LAI_{shade,j}\right) \tag{9}$$

Derivation of sunlit and shaded components of LAI in each layer is based on Norman (1980).

$$LAI_{sun,j} = (T_{B,j} - T_{B,j+1})2\cos\theta \tag{10}$$

$$LAI_{shade,j} = \Delta LAI - LAI_{sun,j} \tag{11}$$

$$T_{B,j} = \exp\left(-\frac{LAI_j}{2\cos\theta}\right) \tag{12}$$

$T_{B,j}$ represents the direct solar beam transmittance below layer j. LAI_j is LAI below layer j. θ is solar zenith angle.

To calculate $g_{s,sun,j}$ and $g_{s,shade,j}$, PAR components on sunlit and shaded leaves in the jth layer ($PAR_{sun,j}$ and $PAR_{shade,j}$, respectively) are used for the derivation of A in Eq. (6). PAR component is calculated based on an assumption that shaded leaves receive only diffused solar radiation and sunlit leaves receive both direct and

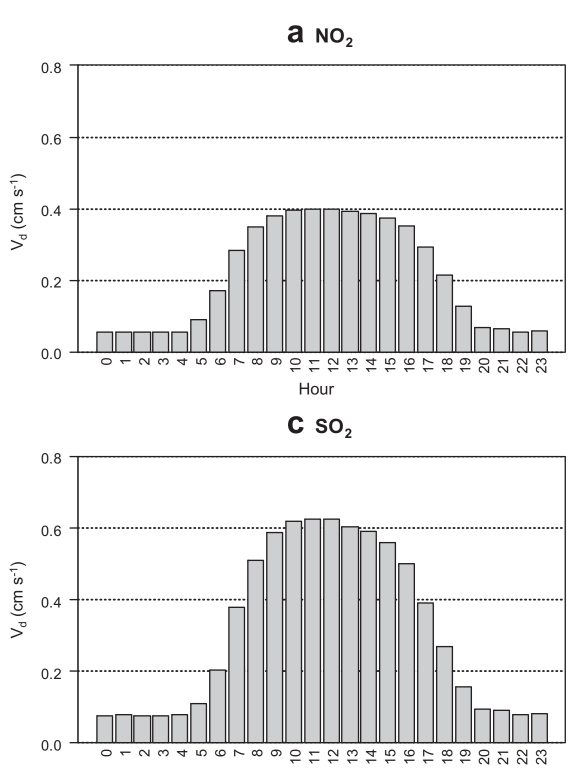

Fig. 2. Hourly estimates of V_d for (a) NO_2, (b) O_3, and (c) SO_2 during leaf-on season in 2005.

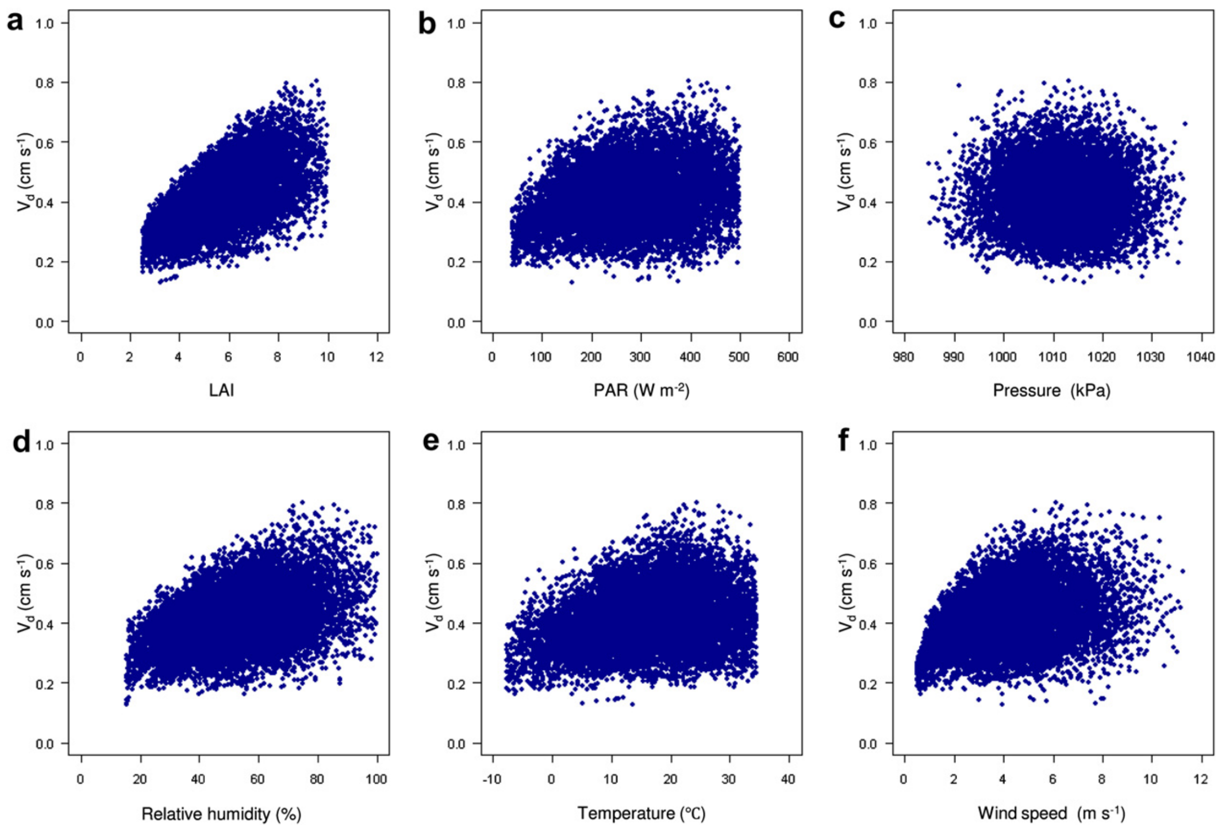

Fig. 3. Scatterplots of V_d for NO_2 and input parameters obtained from the LHS-MC sensitivity analysis.

diffused solar radiation. Norman (1980, 1982) and Baldocchi et al. (1987) describe these processes and solutions in detail. In this study, the scaling factor (S_j) was added to their functions to scale diffused PAR through the canopy layers.

$$\mathrm{PAR}_{\mathrm{shade},j} = \mathrm{PAR}_{\mathrm{diff}} \exp\left(-0.5\mathrm{LAI}^{0.7}\right) S_j + 0.07\mathrm{PAR}_{\mathrm{dir}}\left[1.1 - 0.1\left(\mathrm{LAI}_j - \frac{\Delta\mathrm{LAI}}{2}\right)\right] \exp(-\cos\theta) \quad (13)$$

$$\mathrm{PAR}_{\mathrm{sun},j} = \mathrm{PAR}_{\mathrm{dir}}\frac{\cos\alpha}{\cos\theta} + \mathrm{PAR}_{\mathrm{shade},j} \quad (14)$$

$\mathrm{PAR}_{\mathrm{diff}}$, $\mathrm{PAR}_{\mathrm{dir}}$ are the flux density of diffuse and direct PAR above the canopy, respectively. LAI is leaf area index for the entire canopy, and α is mean angle between leaves and the sun (=60°).

The divisions of solar irradiance into direct and diffuse components as well as into PAR and near-infrared components are based on the method described in Weiss and Norman (1985). PAR is calculated as 46 percent of total solar irradiance (Norman, 1982; Monteith and Unsworth, 1990) that is calculated based on the National Renewable Energy Laboratory Meteorological/Statistical Solar Radiation Model (METSTAT) with inputs from the meteorological data set (Maxwell, 1998).

As removals of CO and PM10 by vegetation are not directly related to transpiration, R_c for CO was set to a constant for the leaf-on season (50,000 s m^{-1}) and the leaf-off season (1,000,000 s m^{-1}) based on data from Bidwell and Fraser (1972). For PM10, the median deposition velocity (Lovett, 1994) was set to 0.0064 m s^{-1} based on a 50-percent resuspension rate of particles back to the atmosphere (Zinke, 1967). The base V_d was adjusted according to actual LAI and a surface-area index for bark of 1.7 (m^2 of bark per m^2 of ground surface covered by the tree crown) (Whittaker and Woodwell, 1967).

Table 3
Pearson product moment correlation coefficient (PMCC) between V_d and each parameter.

Air pollutant	Parameters					
	LAI	PAR	Pressure	Relative humidity	Temperature	Wind speed
NO_2	0.60[a]	0.27[a]	0.001	0.45[a]	0.29[a]	0.34[a]
O_3	0.31[a]	0.33[a]	−0.004	0.54[a]	0.35[a]	0.40[a]
SO_2	0.27[a]	0.33[a]	−0.004	0.56[a]	0.36[a]	0.38[a]

[a] Significantly different than zero at a 5% level.

2.3. Base component

A single run of the original UFORE-D estimates dry deposition for a single air pollutant on an hourly basis and creates a variety of summary output tables. The base component implements exactly the same functions and repeats it five times to process the five air pollutants in a single run. Annual summaries created include total air pollutant removal by dry deposition in the study area, total air pollutant removal per unit tree cover area, and ranges of these values. Monthly summaries include total air pollutant removal by dry deposition for each month, which shows seasonal variation of urban forest effects on air quality. Daily summaries show daily air pollution removal by the entire study area and per unit tree cover area in leaf-on and leaf-off seasons.

2.4. Monte Carlo with Latin hypercube sampling (LHS-MC) component

In the Monte Carlo (MC) analysis, a large number of parameter sets are generated according to the probability density functions of

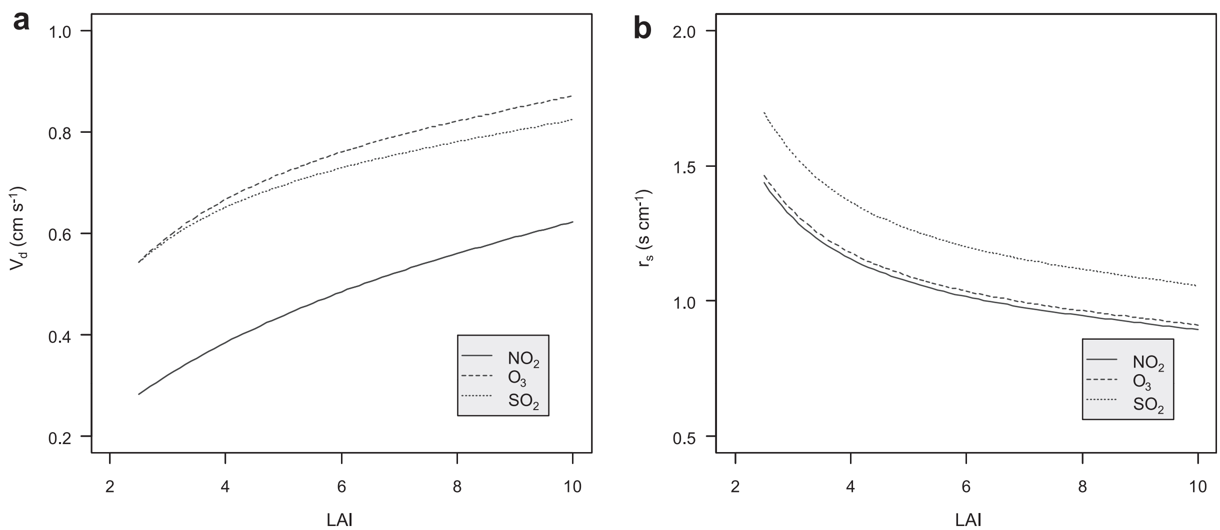

Fig. 4. Results from local sensitivity analysis (a) V_d for NO_2, O_3, and SO_2 against LAI, (b) r_s for NO_2, O_3, and SO_2 against LAI.

the parameters. The model is run with each of these parameter sets, and the results are statistically analyzed. The key to this approach is to apply efficient and unbiased methods for the parameter set selection. In Latin hypercube sampling (LHS) (Saltelli et al., 2000; Zádor et al., 2005; Mészáros et al., 2009), the range of parameters to be varied during the MC simulations is divided into N intervals of equal marginal probability $1/N$, and one sample of each parameter is made at the midpoint of each interval. Thus N non-overlapping values for each input parameter are generated. The parameter values are then randomly grouped to generate N parameter sets. This sampling method ensures that the parameter space is represented with a good approximation of full coverage. Note that this method does not address the cross-correlation between parameter values (i.e. it assumes model parameters are independent).

The LHS-MC component implements this algorithm to perform a sensitivity analysis of V_d estimated by UFORE-D. In this study, hourly meteorological data at noon throughout 2005 (i.e. 365 hourly data for each meteorological parameter) were employed. Using the Meteorology DB Reader, statistics of these 365 hourly meteorological values were extracted (Table 1). Note that the minimum wind speed was set to 0.5 ($m\ s^{-1}$) because extremely small values would mathematically lead to extremely large R_a and R_b in UFORE-D, resulting in an underestimation of V_d. LAI statistics were taken from Breuer et al. (2003). The probability density functions of these input data were assumed to have a normal distribution. The simulation was performed 10,000 times in this study.

In addition, the LHS-MC component supports local sensitivity analyses, in which UFORE-D runs for specific times with only one parameter varied within its possible range and other parameters fixed at their averages. This technique can be used to isolate the effect of the specific parameter on the model output. Hourly meteorological data at noon throughout the year 2005 were used in the local sensitivity analyses.

2.5. Morris one-at-a-time (MOAT) component

In the Morris one-at-a-time (MOAT) method (Morris, 1991; Saltelli et al., 2000; Zádor et al., 2005; van Griensven et al., 2006; Mészáros et al., 2009), $k+1$ parameter sets (where k is the number of parameters) are generated with the algorithm of Morris (1991). In the parameter sets, a given parameter can take exactly two values. In every run, only one parameter is randomly selected and its value is changed compared to the previous run, and every parameter is changed exactly once during the $k+1$ runs. The values of the parameter are selected from the entire range of the parameters by determining a small number of equidistant points. Four equidistant points (minimum, maximum, and two intermediate values) are often used (Morris, 1991; Saltelli et al., 2000; Zádor et al., 2005; Campolongo et al., 2007). The advantage of the Morris method is its computational cheapness, while the parameters are varied across their entire range.

The MOAT component implements this algorithm to perform a sensitivity analysis of V_d estimated by UFORE-D. As with LHS-MS, the analysis was performed with the data at noon throughout 2005, and the minimum and maximum meteorology data were extracted with the Meteorology DB Reader component. In this study, every parameter could take four equidistant values and the procedure was repeated 10 times ($10 \times (k+1)$ runs in total).

The elementary effect (van Griensven et al., 2006; Mészáros et al., 2009), d_i, for the ith input parameter x_i is defined as:

$$d_i = \frac{\frac{y(x_1,\ldots x_i+\Delta,\ldots x_k)-y(x_1,\ldots x_i,\ldots x_k)}{y(x_1,\ldots x_i,\ldots x_k)}}{\frac{\Delta}{x_i}} \quad (15)$$

where Δ is the parameter step size given by the algorithm, x_i is the parameter value to be changed, and y is the model output. The means and standard deviations of d_i give useful information about the influence of the input parameters on the output. A high mean indicates a parameter with an important overall influence on the output. A high standard deviation indicates either a parameter interacting with other parameters or a non-linear effect of the parameter on the output; a low standard deviation indicates the parameter has an approximately linear effect.

3. Study area and data employed

A case study using the three model applications was performed in Baltimore, MD. The center coordinate of the city is 39.17°N and 76.37°W and the area of the city is 209.3 km^2. Tree coverage in Baltimore is 20.4% and the maximum LAI is 4.99. Hourly meteorological data in 2005 was employed from the Baltimore Washington International Airport (BWI) weather station (NCDC, 2008). Air pollution concentration data for 2005 was employed from the United States Environmental Protection Agency's Air Quality System (AQS) (US EPA, 2009).

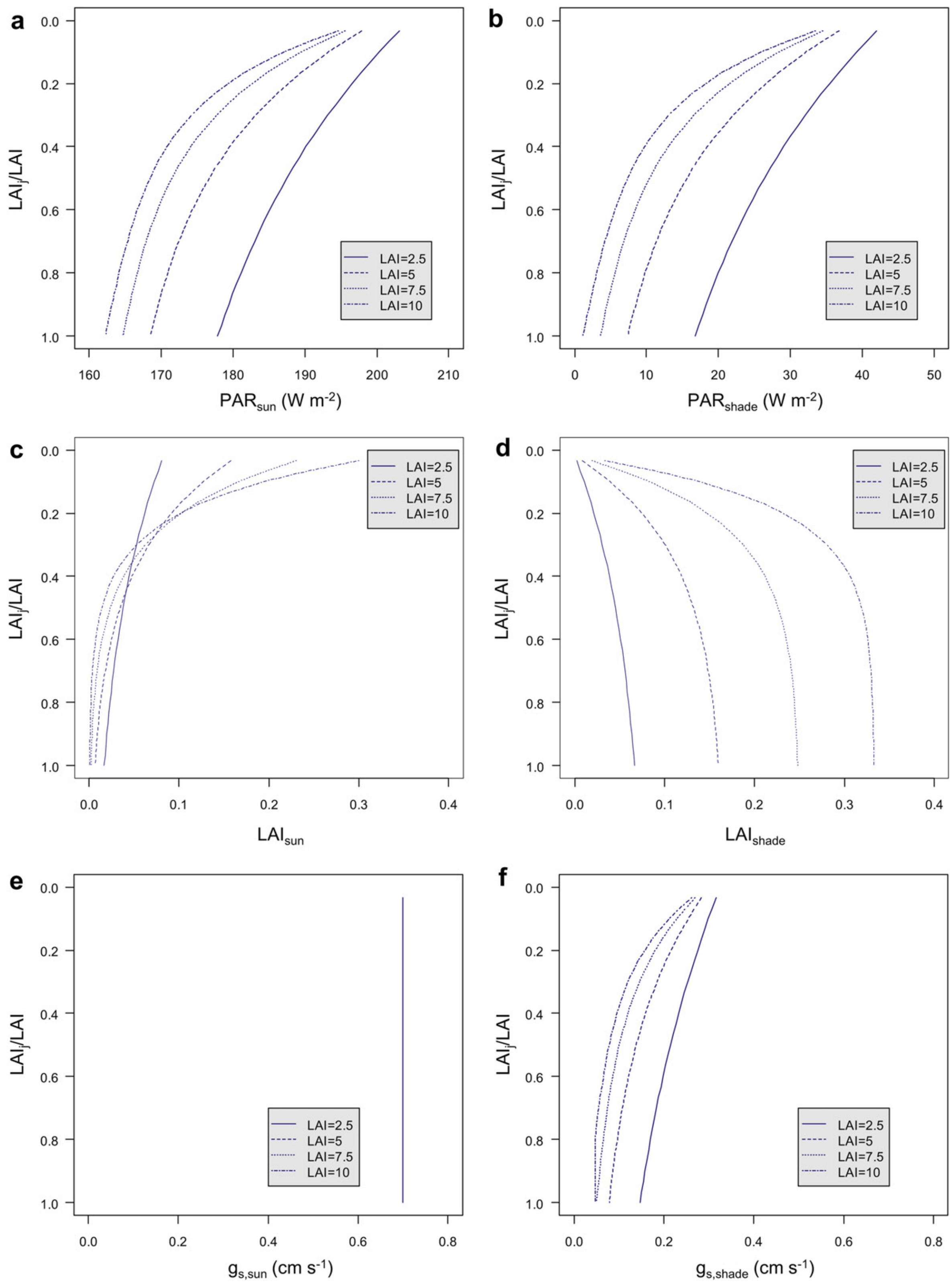

Fig. 5. Vertical profile of (a) PAR_{sun}, (b) PAR_{shade}, (c) LAI_{sun}, (d) LAI_{shade}, (e) $g_{s,sun}$, and (f) $g_{s,shade}$ for LAI = 2.5, 5, 7.5, and 10.

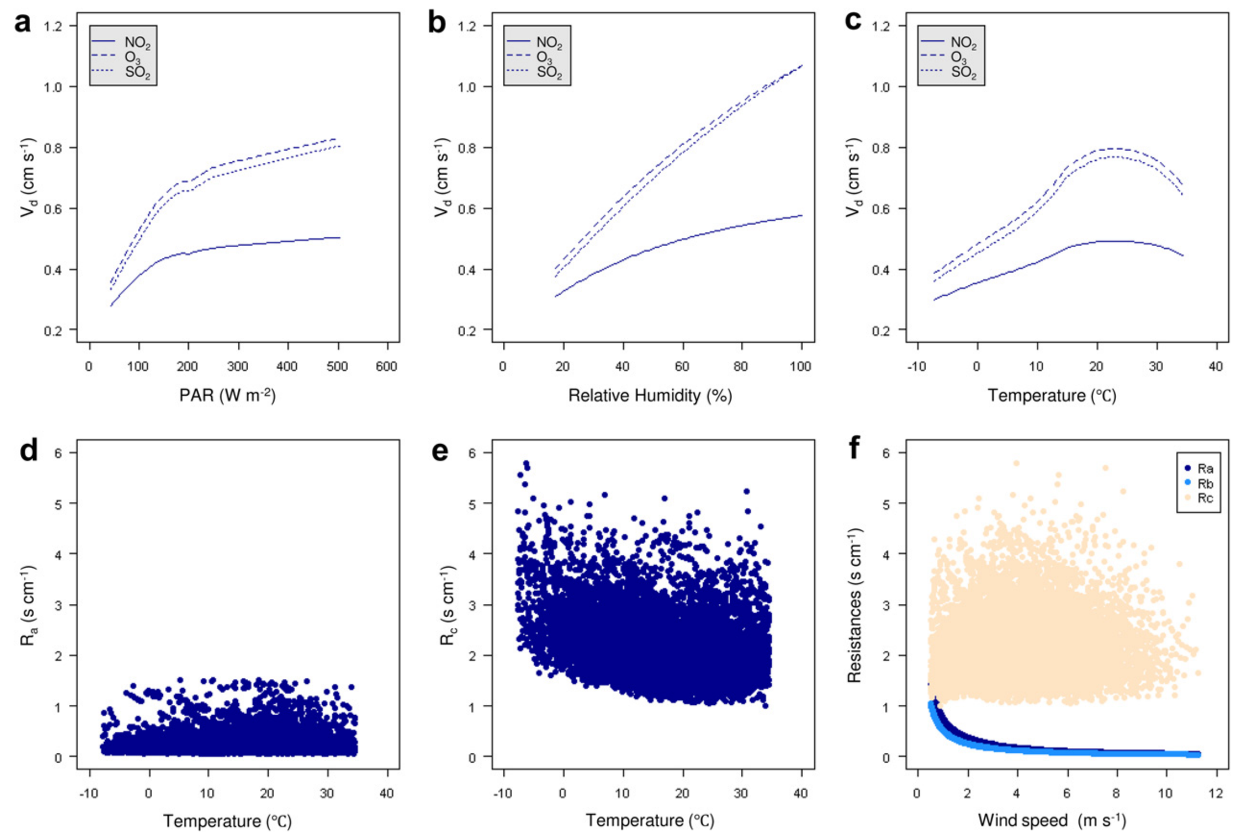

Fig. 6. Results from local sensitivity analysis (a) V_d against PAR, (b) V_d against relative humidity, and (c) V_d against temperature, and scatterplot obtained from LHS-MC for NO_2 (d) R_a against temperature, (e) R_c against temperature, and (f) resistances against wind speed.

4. Results and discussions

4.1. Air pollutant removal

Results obtained from the base application are presented in this section. Table 2 presents annual removal statistics for 2005. Total estimated pollution removal by trees in the study area was 447 metric tons with O_3 (199 t) removed the most and CO (7 t) removed the least. Pollutant removal per unit tree cover area ranged from 0.2 g m^{-2} for CO to 4.7 g m^{-2} for O_3. Total pollutant removal per unit tree cover area was 10.5 g m^{-2} for all five pollutants. These results are comparable to those estimated by Nowak et al. (2006), in which the total pollutant removal by trees was 477 metric tons and total pollutant removal per unit tree cover was 12.1 g m^{-2} for 1994 in Baltimore.

V_d during daytime in the leaf-on seasons for NO_2 typically ranges from 0.1 to 0.5 cm s^{-1} (Lovett, 1994). Daytime V_d for O_3 in the literature normally ranges from 0.3 to 1 cm s^{-1} and averages around 0.7 cm s^{-1} (Greenhut, 1983; Colbeck and Harrison, 1985; Davidson and Wu, 1990). Average daytime leaf-on V_d for SO_2 for forests and trees in the literature typically ranges from 0.2 to 2 cm s^{-1} and averages around 1.0 cm s^{-1} (Garland and Branson, 1977; McMahon and Denison, 1979; Fowler and Cape, 1983; Lovett and Lindberg, 1984; Fowler, 1985; Lorenz and Murphy, 1985; Murphy and Sigmon, 1990). Daytime deposition velocities estimated for the leaf-on season showed good agreements with these values (Fig. 2).

4.2. LHS-MC analysis

The LHS-MC analysis provides a good estimate of the attainable minimum and maximum values of the model outputs (Zádor et al., 2005; Mészáros et al., 2009), while the input parameters change across their possible ranges. This comprehensive approach is the main advantage of this method. One weakness of the method is that it treats the parameters as independent variables, despite the fact that many inputs are highly correlated. For example, relative humidity, temperature, and solar radiation are all highly correlated and have a strong diurnal cycle. However, a wide range of temperature can occur for a given relative humidity and vice versa, and this analysis covers the whole range of realistic values of meteorological parameters in the specific period. Nevertheless, as this sensitivity test is simple and realistic it has been used in various model developments.

A scatterplot between model parameter values and model output is one of the most intuitive and straightforward techniques to provide a qualitative measure of sensitivity (Saltelli et al., 2000). It may reveal relationships between model inputs and outputs, such as non-linear relationships and thresholds (Helton, 1993). Pearson product moment correlation coefficient (PMCC) is another simple measure of sensitivity, which is a measure of the linear relationship between input and output values (Saltelli et al., 2000). Here PMCC is employed to explore the strength of the linear relationship between input and output values.

Since UFORE-D calculates CO and PM10 removals based on constants R_c and V_d, respectively, the results for these pollutants are less affected by meteorological and vegetation parameters. Thus, the analysis presented here is limited to NO_2, O_3, and SO_2. The input parameters analyzed are LAI, PAR, pressure, relative humidity, temperature, and wind speed. Fig. 3 presents scatterplots of V_d for NO_2 and the given input parameter, and Table 3 presents PMCC between V_d and the parameters calculated for NO_2, O_3, and SO_2.

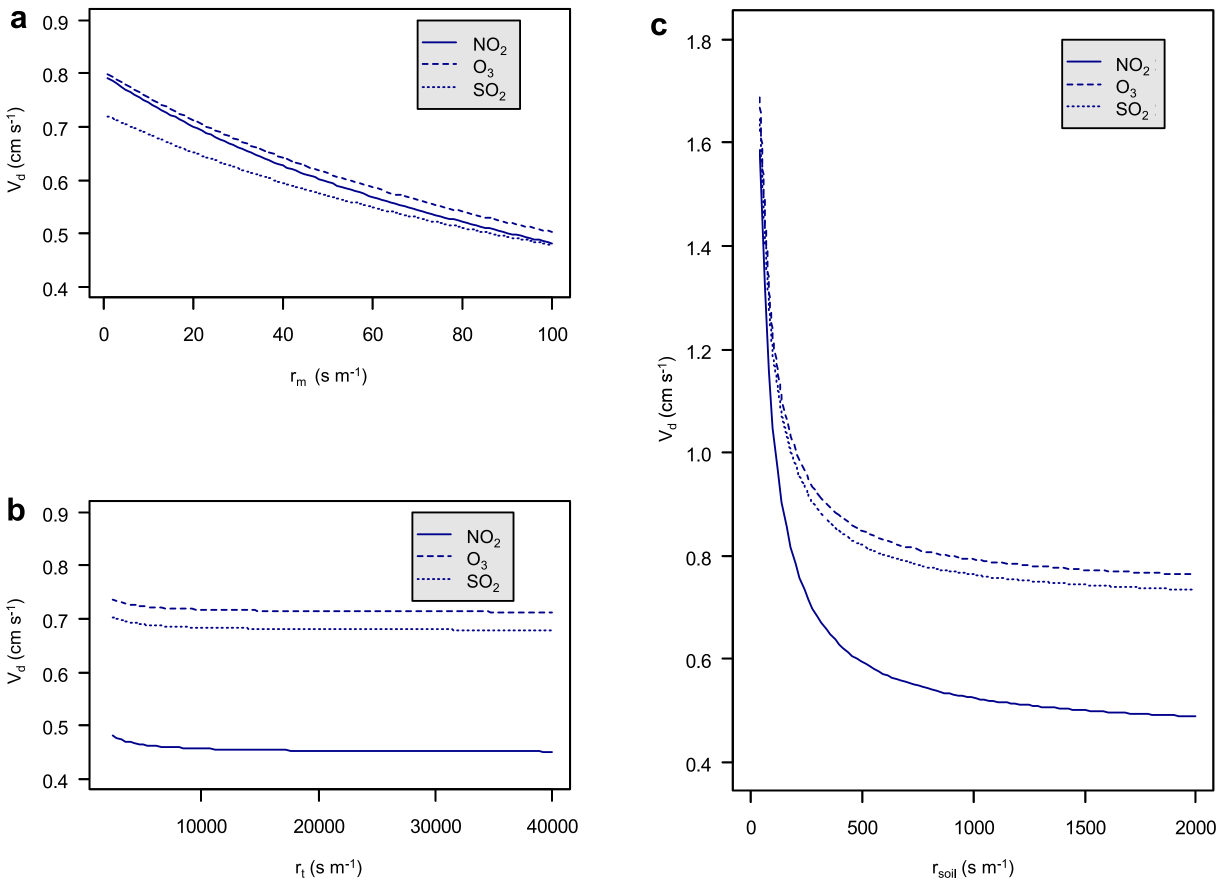

Fig. 7. Results from local sensitivity analysis (a) V_d against r_m, (b) V_d against r_t, and (c) V_d against r_{soil}.

LAI is a major parameter governing the computations of r_m, r_t, and r_s. Based on the scatterplot and the PMCC, LAI has a near linear relationship with V_d for NO_2. PMCCs indicate a smaller linear effect of LAI on V_d for O_3 and SO_2. Employing the same LAI statistics as this study, Mészáros et al. (2009) reported that the deposition velocity of O_3 increased as the LAI increased until a maximum V_d was reached (when LAI is around 6), and a further increase of LAI caused a decrease of V_d. Contrary to this result, the LAI in this study didn't cause a decrease in V_d. To isolate the effect of LAI on the model output, a local sensitivity analysis was performed. In this technique, UFORE-D was run 100 times with only LAI varied within its possible range and other parameters fixed at their averages. Fig. 4(a) shows

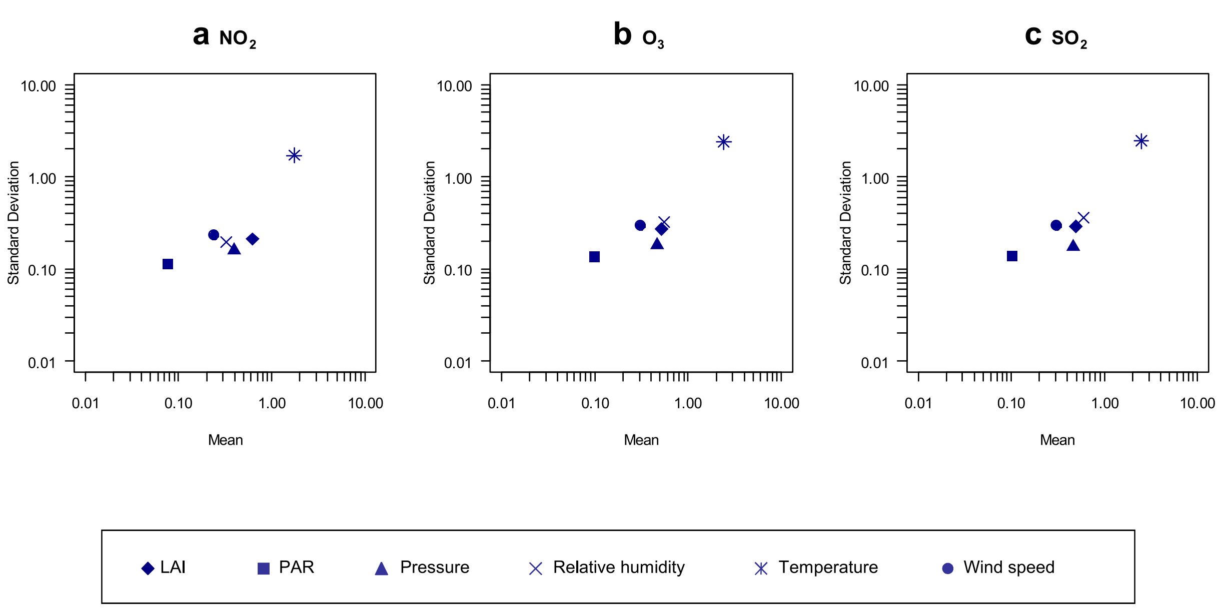

Fig. 8. Mean and standard deviation of elementary effects of each parameter on V_d.

the result for NO_2, O_3, and SO_2 in which V_d increases as LAI increases. This difference was caused due to different calculations of r_s in this study and Mészáros et al.'s (2009). Mészáros et al. (2009) treated the entire canopy as one "big-leaf" and g_s for the entire canopy was represented as a function of average sunlit/shaded LAI and PAR throughout the canopy.

$$g_s = \frac{\mathrm{LAI_{sun}}}{r_s(\mathrm{PAR_{sun}})} + \frac{\mathrm{LAI_{shade}}}{r_s(\mathrm{PAR_{shade}})} \tag{16}$$

As noted in Mészáros et al. (2009), insufficient parameterization of PAR in their study caused a rapid decrease in both PAR_{sun} and PAR_{shade} as LAI increased. For both sunlit and shaded leaves, r_s was determined based solely on PAR and constant values. Therefore, a decrease in PAR directly affected an increase in r_s. In Eq. (16), the magnitude of LAI increase may have been greater than that of r_s increase up to LAI's threshold value of 6, and as a result g_s and V_d increased. When the LAI passed its threshold, however, the magnitude of r_s increase may have become greater than that of LAI increase, and thus g_s and V_d became smaller.

Here we divided the canopy into sublayers and g_s for the canopy was estimated based on values for each layer. Fig. 5(a)–(f) presents vertical profiles of PAR, LAI, and g_s for sunlit and shaded leaves commonly calculated for NO_2, O_3, and SO_2 by our model when LAI = 2.5, 5, 7.5, and 10. The vertical axis, LAI_j/LAI, represents vertical layers of the canopy with 1.0 and near 0.0 representing the bottom and the top of the canopy, respectively. As shown in Fig. 5(a) and (b), both PAR_{sun} and PAR_{shade} in each layer decreased as LAI increased, but in much smaller magnitude than Mészáros et al.'s (2009). LAI_{sun} was larger near the top of the canopy for larger LAI, though near the canopy bottom LAI_{sun} became smaller (Fig. 5(c)) since fewer leaves receive direct sunlight due to denser upper leaves; LAI_{shade} increased as LAI increased, especially at the bottom of the layer (Fig. 5(d)). $g_{s,sun}$ was estimated as constant for sunlit leaves (Fig. 5(e)) regardless of LAI and canopy layers, whereas $g_{s,shade}$ decreased for larger LAI (Fig. 5(f)). With Eq. (9), g_s was weighted with LAI for sunlit/shaded leaves in each layer and summed up throughout the layers to estimate g_s for the entire canopy. As a result, r_s for the entire canopy was estimated as shown in Fig. 4(b). Although the magnitude of r_s decrease got smaller with larger LAI, r_s never increased. Similarly, the magnitude of V_d increase became smaller as LAI increased, though a decrease in V_d did not occur (Fig. 4(a)).

PAR has an important role in determining V_d by influencing the opening and closing of leaf stomata (Brook et al., 1999). PAR on the top of the canopy is divided into PAR_{sun} and PAR_{shade} in each layer to estimate r_s. The scatterplot (Fig. 3(b)) indicates a non-linear effect of the PAR on V_d for NO_2. O_3 and SO_2 exhibited similar results (not shown here). The local sensitivity analysis of PAR for NO_2 showed that V_d increased as PAR increased until around 300–400 W m^{-2} (Fig. 6 (a)). This result agrees with the study by Brook et al. (1999), which reported that once the stomata were open the magnitude of PAR became less important for V_d (i.e. stomatal opening peaked with relatively low levels of PAR). Wu et al. (2003) estimated that plants reach their light saturation point at about 800 W m^{-2} of global solar radiation. As PAR is calculated as 46 percent of the global solar radiation (Norman, 1982; Monteith and Unsworth, 1990), this threshold is equivalent to a PAR of 368 W m^{-2}, and is in good agreement with the result presented here.

As can be seen in Fig. 3(c), (d), and Table 3, pressure, which affects r_s through the computation of solar radiation components, PAR_{dir} and PAR_{diff} appeared to have no relationship with V_d. Relative humidity, which influences r_s through the derivation of g_s, had a near linear effect on V_d. Wu et al. (2003) analyzed the effects of relative humidity ranging from 0 to 100% on the flux of O_3 and SO_2. The flux increased non-linearly with larger relative humidity until it reached a maximum at a relative humidity of 100%. As shown in Fig. 6(b), a similar behavior as reported by Wu et al. (2003) was observed in our local sensitivity analysis.

Temperature appeared to have a non-linear effect on V_d based on the scatterplot in Fig. 3(e). Temperature is used to calculate all three resistances in Eq. (2). To examine the effect of temperature on each resistance, resistances calculated in the LHS-MC analysis were plotted in Fig. 6(d) and (e). R_a and R_b appeared to vary independent of temperature, and the magnitude of variability was smaller than that of R_c. R_c had larger variability, and seemed to decrease as temperature rose up to around 20 (°C) and increased afterwards. Fig. 6(c) shows the change in V_d against the change in temperature obtained by the local sensitivity analysis. V_d increased as temperature increased until about 20 °C, and further increases in temperature caused decreases in V_d. This result indicates that the maximum V_d occurs at an optimal temperature where the stomatal conductance is not limited (Wu et al., 2003; Mészáros et al., 2009).

Fig. 3(f) suggested that the relationship between V_d and wind speed was not linear. In this figure, the distribution can be divided into plots for the minimum to 2 m s^{-1} of wind speed, where V_d rapidly increased, and plots for wind speed larger than 2 m s^{-1}, where V_d gradually increased. Wind speed primarily affects R_a and R_b; the increase in turbulence that accompanies increasing wind speeds resulted in decreased R_a, whereas the increase in friction velocity due to the increase in wind speed resulted in decreased R_b. Fig. 6(f) presents scatterplots between wind speed and R_a, R_b, and R_c. When the wind speed was less than 2 m s^{-1}, large R_a and R_b were dominant in determining the small V_d values shown in Fig. 3 (f), and these resistances rapidly decreased as wind speed increased. R_c didn't appear to be affected by wind.

In several models, r_m, r_t, and r_{soil} are parameterized with a constant value. The range of r_m for the three air pollutants is typically from 0 to 100 s m^{-1} (Hosker and Lindberg, 1982; Baldocchi, 1988; Wesely, 1989; Zhang et al., 2002). r_t is typically set to much larger values, and ranges from 20,000 to 40,000 s m^{-1} for NO_2 (Wesely, 1989; Mészáros et al., 2009), from 2000 to 10,000 s m^{-1} for O_3 (Wesely, 1989; Zhang et al., 2003), and from 2000 to 8000 s m^{-1} for SO_2 (Baldocchi, 1988; Wesely, 1989; Zhang et al., 2003). Typical r_{soil} for the three air pollutants is from 20 to 2000 s m^{-1} (Hosker and Lindberg, 1982; Baldocchi, 1988; Meyers and Baldocchi, 1993; Zhang et al., 2003). UFORE-D also employed constant values for r_m, r_t, and r_{soil}. To explore the effects of these resistances on V_d, local sensitivity analyses were performed, in which only one resistance value varied across its possible range, the other resistances remained at their constant value, and other parameters fixed at their average values presented in Table 1. r_m, r_t, and r_{soil} determine R_c (Eq. (5)), which in turn determines V_d (Eq. (2)). Fig. 7 presents the results for NO_2, O_3, and SO_2. In general, the constant values set to each resistance had a large effect on determining the typical value of V_d. For example in Fig. 7(a), r_m for NO_2, O_3, and SO_2 was set to 100 s m^{-1}, 10 s m^{-1}, and 0 s m^{-1}, respectively. Corresponding V_d is 0.48 cm s^{-1}, 0.75 cm s^{-1}, and 0.72 cm s^{-1}, respectively, which are close to the hourly average V_d at noon for the leaf-on season (Fig. 2). Choosing different values for the resistances will impact V_d; however, each resistance has a varied impact. Within the possible range of r_m, decrease in V_d for NO_2, O_3, and SO_2 was relatively large (39%, 37%, and 34%, respectively). Contrarily, changes in r_t caused very small changes in V_d because its value is much larger than r_m, and thus, the effect of r_t on the model output was minimal. Over the possible range of r_{soil}, V_d decreased rapidly as r_{soil} increased up to about 1000 s m^{-1}, then after this value decreases in V_d became much smaller. Overall, the decrease in V_d for NO_2, O_3, and SO_2 (69%, 55%, and 55%, respectively) was largest among the three resistances. While the constant values for r_{soil}

employed in UFORE-D (2000 s m^{-1} for the three air pollutants) is at the high end of the r_{soil} range, other models have employed smaller values such as 20–200 s m^{-1} (Hosker and Lindberg, 1982), 300 s m^{-1} (Baldocchi, 1988), and 50–500 s m^{-1} (Zhang et al., 2003) depending on soil moisture and vegetation. As r_{soil} plays an important role in the model, further investigation of this model parameter is necessary to improve the quality of UFORE-D.

4.3. MOAT analysis

While the LHS-MC analysis presents accurate and unbiased information about the sensitivity of model outputs to changes in model inputs, it does not quantify the variability of the output based on the variability of individual parameters. The Morris method, on the other hand, provides individual effects of the parameters on the modeled V_d. Two sensitivity measures for each input parameter can be obtained: mean of the elementary effect, indicating the overall impact of input variability on output variability, and standard deviation of the elementary effect, indicating non-linearity or interaction effects.

Fig. 8 presents results from the Morris method, in which the means and the standard deviations of the elementary effect of each parameter are plotted against each other (note that both scales are logarithmic). A higher mean indicates a greater effect of the parameter on V_d. A lower standard deviation denotes a linear effect. Temperature had the greatest mean and standard deviation, indicating its large impact on model output and the non-linear relationship between temperature and V_d for all pollutants. LAI was among the second most important parameters for the three air pollutants. The linearity of LAI and V_d is stronger for NO_2 than for the other two pollutants. Mean of wind speed and PAR was found among the smallest mean, indicating the smallest impact on the model output.

5. Conclusions

In this study, UFORE-D was redeveloped into a set of COM components. Reusing the developed components, two applications were developed to examine the sensitivity of UFORE-D to its input parameters. Based on the component-based model development and results from the sensitivity analyses, the following conclusions can be drawn:

1. Building new applications upon UFORE-D could be efficiently achieved if UFORE-D consisted of reusable components. It was not necessary to learn and modify the source codes; instead, newly developed components only needed to communicate with existing components through appropriate interfaces (class, methods, and parameters).
2. Component-based UFORE-D readily accepted new data formats. Employing new data formats only required replacing the old components with ones that handle the new data formats.
3. UFORE-D output revealed different sensitivity to input parameters depending on the specific air pollutants. However, temperature was commonly important for the modeling process and its effect was non-linear. Dry deposition velocity (V_d) increased as temperature increased until it reached its maximum value at a threshold temperature (here ∼20 °C). Above the threshold V_d decreased as temperature increased.
4. Among the three resistances used to determine V_d, the effect of temperature appeared to be greater on canopy resistance (R_c) than on aerodynamic resistance (R_a) and quasi-laminar boundary layer resistance (R_b).
5. Among the parameters affecting R_c, LAI was important for dry deposition of NO_2, O_3, and SO_2. The linear effect of LAI on V_d is stronger for NO_2 than O_3 and SO_2. PAR was only influential up to its threshold (here 300–400 W m^{-2}) at which the stomata were fully open. Pressure and relative humidity were less important in the dry deposition process.
6. Wind speed was influential to the computation of R_a and R_b; however, the effect was dominant only when the wind speed was less than its threshold (here 2 m s^{-1}). Larger wind speed had smaller effects on the dry deposition process.
7. Soil (r_{soil}) and mesophyll resistances (r_m) exhibited a large effect on the dry deposition process. The effect of cuticular resistance (r_t) on the dry deposition process was very limited due to its large magnitude.

The component design of this study allows users to reuse core functions of UFORE-D, in which submodels to estimate resistances for pollutant transfer are implemented and V_d is estimated by combining these results. If users need to extend the core functions of UFORE-D, it is required for them to learn and modify source codes of the Dry Deposition component. Therefore, one potential future work is to further separate the Dry Deposition component into smaller components, such as ones for calculating R_a, R_b, and r_s. Depending on component designs, component-based modeling can provide more flexibility and extendability to models, which can lead to more efficient and effective model developments.

UFORE-D is composed of a large number of relations among meteorological as well as vegetation parameters (see Hirabayashi et al. (2010) for the full description of the model). To explore the sensitivity of such complex models, Monte Carlo and Morris sensitivity analyses employed in this study are a good preliminary technique (Norman, 2008). One future direction of the model study includes further investigation of the most important relations identified by this study using the algebraic sensitivity analysis (Norman, 2008).

References

Alonso, G., Casati, F., Kuno, H., Machiraju, V., 2004. Web Services: Concepts, Architectures and Applications. Springer-Verlag, New York.

Anfossi, D., Sacchettit, D., Castelli, S.T., 1996. Development and sensitivity analysis of a Lagrangian particle model for long range dispersion. Environmental Software 10 (4), 263–287.

Argent, R.M., 2004. An overview of model integration for environmental applications – components, frameworks and semantics. Environmental Modelling & Software 19 (3), 219–234.

Baldocchi, D., 1988. A multi-layer model for estimating sulfur dioxide deposition to a deciduous oak forest canopy. Atmospheric Environment 22 (5), 869–884.

Baldocchi, D., 1994. An analytical solution for coupled leaf photosynthesis and stomatal conductance models. Tree Physiology 14, 1069–1079.

Baldocchi, D.D., Hicks, B.B., Camara, P., 1987. A canopy stomatal resistance model for gaseous deposition to vegetated surfaces. Atmospheric Environment 21 (1), 91–101.

Baldocchi, D.D., Harley, P.C., 1995. Scaling carbon dioxide and water vapour exchange from leaf to canopy in a deciduous forest. II. Model testing and application. Plant, Cell and Environment 18 (10), 1157–1173.

Baldocchi, D.D., Wilson, K.B., 2001. Modeling CO_2 and water vapor exchange of a temperate broadleaved forest across hourly to decadal time scales. Ecological Modelling 142 (1–2), 155–184.

Barnsley, M.J., 2007. Environmental Modeling: A Practical Introduction. CRC Press, Boca Raton, FL.

Bian, L., 2000. Component modeling for the spatial representation of wildlife movements. Journal of Environmental Management 59 (4), 235–245.

Bidwell, R.G., Fraser, D.E., 1972. Carbon monoxide uptake and metabolism by leaves. Canadian Journal of Botany 50 (7), 1435–1439.

Breuer, L., Eckhardt, K., Frede, H.-G., 2003. Plant parameter values for models in temperate climates. Ecological Modelling 169 (2–3), 237–293.

Brook, J.R., Zhang, L., Li, Y., Johnson, D., 1999. Description and evaluation of a model of deposition velocities for routine estimates of dry deposition over North America. Part II: Review of past measurements and model results. Atmospheric Environment 33 (30), 5053–5070.

Campolongo, F., Saltelli, A., 1997. Sensitivity analysis of an environmental model: an application of different analysis methods. Reliability Engineering & System Safety 57, 49–69.

Campolongo, F., Cariboni, J., Saltelli, A., 2007. An effective screening design for sensitivity analysis of large models. Environmental Modelling & Software 22 (10), 1509–1518.

Caton, B.P., Foin, T.C., Hill, J.E., 1999. A plant growth model for integrated weed management in direct-seeded rice I. Development and sensitivity analyses of monoculture growth. Field Crops Research 62 (2–3), 129–143.

Chappell, D., 1996. Understanding ActiveX and OLE: A Guide for Developers & Managers. Microsoft Press, Redmond, WA.

Colbeck, I., Harrison, R.M., 1985. Dry deposition of ozone: some measurements of deposition velocity and of vertical profiles to 100 meters. Atmospheric Environment 19 (11), 1807–1818.

Collatz, G.J., Ball, J.T., Grivet, C., Berry, J.A., 1991. Physiological and environmental regulation of stomatal conductance, photosynthesis and transpiration: a model that includes a laminar boundary layer. Agricultural and Forest Meteorology 54 (2–4), 107–136.

Currie, B.A., Bass, B., 2008. Estimates of air pollution mitigation with green plants and green roofs using the UFORE model. Urban Ecosystems 11 (4), 409–422.

Davidson, C.I., Wu, Y.L., 1990. Dry deposition of particles and vapors. In: Lindberg, S.E., Page, A.L., Norton, S.A. (Eds.), Acidic Precipitation. Sources, Deposition, and Canopy Interactions, vol. 3. Springer-Verlag, New York, pp. 103–216.

Deutsch, B., Whitlow, H., Sullivan, M., Savineau, A., 2005. Re-greening Washington, DC: A Green Roof Vision Based on Quantifying Storm Water and Air Quality Benefits. http://www.greenroofs.org/resources/greenroofvisionfordc.pdf (accessed February 2009).

Dyer, A.J., Bradley, C.F., 1982. An alternative analysis of flux gradient relationships. Boundary-Layer Meteorology 22 (1), 3–19.

Farquhar, G.D., von Caemmerer, S., Berry, J.A., 1980. A biochemical model of photosynthetic CO_2 assimilation in leaves of C3 species. Planta 149 (1), 78–90.

Fowler, D., 1985. Deposition of SO_2 onto plant canopies. In: Winner, W.E., Mooney, H.A., Goldstein, R.A. (Eds.), Sulfur Dioxide and Vegetation. Stanford University Press, Stanford, CA, pp. 389–402.

Fowler, D., Cape, J.N., 1983. Dry deposition of SO_2 onto a Scots pine forest. In: Pruppacher, H.R., Semonin, R.G., Slinn, W.G.N. (Eds.), Precipitation Scavenging, Dry Deposition and Resuspension. Elsevier, New York, pp. 763–773.

Garland, J.A., Branson, J.R., 1977. The deposition of sulfur dioxide to pine forest assessed by a radioactive tracer method. Tellus 29, 445–454.

Greenhut, G.K., 1983. Resistance of a pine forest to ozone uptake. Boundary-Layer Meteorology 27 (4), 387–391.

Hamby, D.M., 1994. A review of techniques for parameter sensitivity analysis of environmental models. Environmental Monitoring and Assessment 32, 135–154.

Harley, P.C., Thomas, R.B., Reynolds, J.F., Strain, B.R., 1992. Modelling photosynthesis of cotton grown in elevated CO_2. Plant, Cell and Environment 15 (3), 271–282.

Harley, P.C., Baldocchi, D.D., 1995. Scaling carbon dioxide and water vapour exchange from leaf to canopy in a deciduous forest. I. Leaf model parameterization. Plant, Cell and Environment 18 (10), 1146–1156.

He, C., Larsen, D.R., Mladenoff, D.J., 2002. Exploring component-based approaches in forest landscape modeling. Environmental Modelling & Software 17 (6), 519–529.

Helton, J.C., 1993. Uncertainty and sensitivity analysis techniques for use in performance assessment for radioactive waste disposal. Reliability Engineering & Systems Safety 42 (2–3), 327–367.

Hermann, A.J., Stabeno, P.J., Haidvogel, D.B., Musgrave, D.L., 2002. A regional tidal/subtidal circulation model of the southeastern Bering Sea: development, sensitivity analyses and hindcasting. Deep-Sea Research II 49 (26), 5945–5967.

Hosker Jr., R.P., Lindberg, S.E., 1982. Review: atmospheric deposition and plant assimilation of gases and particles. Atmospheric Environment 16 (5), 889–910.

Hirabayashi, S., Kroll, C.N., Nowak, D.J., 2010. UFORE-D Model Descriptions. http://www.itreetools.org/resources/archives.php (accessed August 2010).

Killus, J.P., Meyer, J.P., Durran, D.R., Anderson, G.E., Jerskey, T.N., Reynolds, S.D., Ames, J., 1984. Continued research in mesoscale air pollution simulation modeling. In: Refinements in Numerical Analysis, Transport, Chemistry, and Pollutant Removal, vol. V. United States Environmental Protection Agency, Research Triangle Park, NC. Publ. EPA/600/3.84/095a.

Leuning, R., 1990. Modelling stomatal behavior and photosynthesis of eucalyptus grandis. Australian Journal of Plant Physiology 17 (2), 159–175.

Liepmann, D., Stephanopoulos, G., 1985. Development and global sensitivity analysis of a closed ecosystem model. Ecological Modelling 30 (1–2), 13–47.

Lorenz, R., Murphy, C.E., 1985. The dry deposition of sulfur dioxide on a loblolly pine plantation. Atmospheric Environment 19 (5), 797–802.

Lovett, G.M., 1994. Atmospheric deposition of nutrients and pollutants in North America: an ecological perspective. Ecological Applications 4 (4), 629–650.

Lovett, G.M., Lindberg, S.E., 1984. Dry deposition and canopy exchange in a mixed oak forest as determined by analysis of throughfall. Journal of Applied Ecology 21 (3), 1013–1027.

MacDougall, M., Smith, R.I., Scott, E.M., 2005. Comprehensive sensitivity analysis of an SO_2 deposition model for three measurement sites: consequences for SO_2 deposition fluxes. Atmospheric Environment 39, 5025–5039.

MacKerron, D.K.L., Waister, P.D., 1985. A simple model of potato growth and yield. Part I. Model development and sensitivity analysis. Agricultural and Forest Meteorology 34 (2–3), 241–252.

Maxwell, E.L., 1998. METSTAT – the solar radiation model used in the production of the national solar radiation database (NSRDB). Solar Energy 62 (4), 263–279.

McMahon, T.A., Denison, P.J., 1979. Empirical atmospheric deposition parameters – a survey. Atmospheric Environment 13, 571–585.

Mészáros, R., Zsély, I.Gy., Szinyei, D., Vincze, Cs, Lagzi, I., 2009. Sensitivity analysis of an ozone deposition model. Atmospheric Environment 43 (3), 663–672.

Meyers, T.P., Baldocchi, D.D., 1993. Trace gas exchange above the floor of a deciduous forest 2. SO_2 and O_3 deposition. Journal of Geophysical Research 98 (D7), 12631–12638.

Microsoft Developer Network (MSDN), 2009. COM Clients and Servers. http://msdn.microsoft.com/en-us/library/ms683835(VS.85).aspx (accessed March 2009).

Monteith, J.L., Unsworth, M.H., 1990. Principles of Environmental Physics. Edward Arnold, New York.

Morris, M.D., 1991. Factorial sampling plans for preliminary computational experiments. Technometrics 33 (2), 161–174.

Murphy, C.E., Sigmon, J.T., 1990. Dry deposition of sulfur and nitrogen oxide gases to forest vegetation. In: Lindberg, S.E., Page, A.L., Norton, S.A. (Eds.), Acidic Precipitation. Sources, Deposition, and Canopy Interactions, vol. 3. Springer-Verlag, New York, pp. 217–240.

National Aeronautics and Space Administration (NASA), 2009. Remote Sensing Tutorial, Section 3 Vegetation Applications – Agriculture, Forestry, and Ecology. http://rst.gsfc.nasa.gov/Sect3/Sect3_1.html (accessed January 2009).

National Climate Data Center (NCDC), 2008. World's Largest Archive of Climate Data: National Climate Data Center. http://www.ncdc.noaa.gov/oa/ncdc.html (accessed September 2008).

National Oceanic & Atmospheric Administration (NOAA), 2010. Trends in Atmospheric Carbon Dioxide – Globally Averaged Marine Surface Annual Mean Data. ftp://ftp.cmdl.noaa.gov/ccg/co2/trends/co2_annmean_gl.txt (accessed November 2010).

Norman, J.M., 1980. Interfacing leaf and canopy light interception models. In: Hesketh, J.D., Jones, J.W. (Eds.), Predicting Photosynthesis for Ecosystem Models, vol. II. CRC Press, Boca Raton, FL, pp. 49–67.

Norman, J.M., 1982. Simulation of microclimates. In: Biometeorology in Integrated Pest Management, 65–99. Proceedings of a Conference on Biometeorology and Integrated Pest Management, Davis, CA.

Norton, J.P., 2008. Algebraic sensitivity analysis of environmental models. Environmental Modelling & Software 23, 963–972.

Nowak, D.J., McHale, P.J., Ibarra, M., Crane, D., Stevens, J., Luley, C., 1998. Modeling the effects of urban vegetation on air pollution. In: Gryning, S.E., Chaumerliac, N. (Eds.), Air Pollution Modeling and its Application XII. Plenum Press, New York, pp. 399–407.

Nowak, D.J., Crane, D.E., 2000. The urban forest effects (UFORE) model: quantifying urban forest structure and functions. In: Hansen, M., Burk, T. (Eds.), Integrated Tools for Natural Resources Inventories in the 21st Century: Proceedings of the IUFRO Conference. United States Department of Agriculture, Forest Service, North Central Research Station, St. Paul, MN, pp. 714–720. Gen. Tech. Rep. NC-212.

Nowak, D.J., Civerolo, K.L., Rao, S.T., Sistla, G., Juley, C.J., Crane, D.E., 2000. A modeling study of the impact of urban trees on ozone. Atmospheric Environment 34 (10), 1601–1613.

Nowak, D.J., Crane, D.E., Stevens, J.C., 2006. Air pollution removal by urban trees and shrubs in the United States. Urban Forestry & Urban Greening 4 (3–4), 115–123.

Pataki, D.E., Bowling, D.R., Ehleringer, J.R., 2003. Seasonal cycle of carbon dioxide and its isotopic composition in an urban atmosphere: anthropogenic and biogenic effects. Journal of Geophysical Research 108 (D23) ACH 8–1–ACH 8–8.

Pederson, J.R., Massman, W.J., Mahrt, L., Delany, A., Oncley, S., Hartog, G.den, Neumann, H.H., Mickle, R.E., Shaw, R.H., Paw, U.K.T., Grantz, D.A., MacPherson, J.I., Desjardins, R., Schuepp, P.H., Pearson Jr., R., Arcado, T.E., 1995. California ozone deposition experiment: methods, results, and opportunities. Atmospheric Environment 29 (21), 3115–3132.

Pohlert, T., Huisman, J.A., Breuer, L., Frede, H.-G., 2007. Integration of a detailed biogeochemical model into SWAT for improved nitrogen predictions—model development, sensitivity, and GLUE analysis. Ecological Modelling 203 (3–4), 215–228.

Ravalico, J.K., Maier, H.R., Dandy, G.C., Norton, J.P., Croke, B.F.W., 2005. A comparison of sensitivity analysis techniques for complex models for environment management. In: Zerger, A., Argent, R.M. (Eds.), International Congress on Modelling and Simulation: Advances and Applications for Management and Decision Making, Melbourne, 12–15 December, pp. 2533–2539.

Saltelli, A., Chan, K., Scot, E.M., 2000. Sensitivity Analysis. John Wiley & Sons, West Sussex, UK.

Simpson, D., Touvinen, J.P., Emberson, L., Ashmore, M.R., 2003. Characteristics of an ozone deposition module II: sensitivity analysis. Water, Air, and Soil Pollution 143, 123–137.

Smith, R.I., Fowler, D., Sutton, M.A., Flechard, C., Coyle, M., 2000. Regional estimation of pollutant gas dry deposition in the UK: model description, sensitivity analyses and outputs. Atmospheric Environment 34, 2757–3777.

Taylor Jr., G.E., Hanson, P.J., Baldocchi, D.D., 1988. Pollutant deposition to individual leaves and plant canopies: sites of regulation and relationship to injury. In: Heck, W.W., Taylor, O.C., Tingey, D.T. (Eds.), Assessment of Crop Loss From Air Pollutants. Elsevier Applied Science, London, England, pp. 227–258.

United States Environmental Protection Agency (US EPA), 1995. PCRAMMET User's Guide. United States Environmental Protection Agency, Research Triangle Park, NC.

United States Environmental Protection Agency (US EPA), 2009. Technology Transfer Network (TTN): Air Quality System (AQS). http://www.epa.gov/ttn/airs/airsaqs/ (accessed February 2009).
van Griensven, A., Meixner, T., Grunwald, S., Bishop, T., Diluzio, M., Srinivasan, R., 2006. A global sensitivity analysis tool for the parameters of multi-variable catchment models. Journal of Hydrology 324 (1–4), 10–23.
van Ulden, A.P., Holtslag, A.A.M., 1985. Estimation of atmospheric boundary layer parameters for diffusion application. Journal of Climatology and Applied Meteorology 24 (11), 1196–1207.
Venkatram, A., 1980. Estimating the Monin-Obukhov length in the stable boundary layer for dispersion calculations. Boundary-Layer Meteorology 19 (4), 481–485.
Vitousek, P.M., Mooney, H.A., Lubchenco, J., Melillo, J.M., 1997. Human domination of earth's ecosystems. Science 277, 494–499.
Weiler, M., 2005. An infiltration model based on flow variability in macropores: development, sensitivity analysis and applications. Journal of Hydrology 310 (1–4), 294–315.
Weiss, A., Norman, J.M., 1985. Partitioning solar radiation into direct and diffuse, visible and near-infrared components. Agricultural and Forest Meteorology 34 (2–3), 205–213.
Wesely, M.L., 1989. Parameterization of surface resistances to gaseous dry deposition in regional-scale numerical models. Atmospheric Environment 23 (6), 1293–1304.
Whittaker, R.H., Woodwell, G.M., 1967. Surface area relations of woody plants and forest communities. American Journal of Botany 54 (8), 931–939.
Wilson, K.B., Baldocchi, D.D., Hanson, P.J., 2001. Leaf age affects the seasonal pattern of photosynthetic capacity and net ecosystem exchange of carbon in a deciduous forest. Plant, Cell and Environment 24 (6), 571–583.
Wu, Y., Brashers, B., Finkelstein, P.L., Pleim, J.E., 2003. A multilayer biochemical dry deposition model 2. Model evaluation. Journal of Geophysical Research 108 (1) ACH2–1 – ACH2–16.
Zádor, J., Zsély, I.Gy., Turányi, T., Ratto, M., Tarantola, S., Saltelli, A., 2005. Local and global uncertainty analyses of a methane flame model. Journal of Physical Chemistry 109 (43), 9795–9807.
Zhang, L., Moran, M.D., Makar, P.A., Brook, J.R., Gong, S., 2002. Modelling gaseous dry deposition in AURAMS: a unified regional air-quality modelling system. Atmospheric Environment 36 (3), 537–560.
Zhang, L., Brook, J.R., Vet, R., 2003. A revised parameterization for gaseous dry deposition in air-quality models. Atmospheric Chemistry and Physics 3 (6), 2067–2082.
Ziehn, T., Tomlin, A.S., 2008. Global sensitivity analysis of a 3D street canyon model—Part I: The development of high dimensional model representations. Atmospheric Environment 42 (8), 1857–1873.
Zinke, P.J., 1967. Forest interception studies in the United States. In: Sopper, W.E., Lull, H.W. (Eds.), Forest Hydrology. Pergamon Press, Oxford, UK, pp. 137–161.